Magnetic Moment of Helium in Its $^3S_1$ Metastable State*†

C. W. DRAKE,‡ V. W. HUGHES, A. LURIO,§ AND J. A. WHITE
Yale University, New Haven, Connecticut

(Received July 30, 1958)

The ratio of the electronic g_J value of He in its $1s2s$, $^3S_1$ metastable state to the g_J of H in its ground state has been redetermined by the atomic beam magnetic resonance method using separated oscillating fields. At magnetic fields of about 540 and 575 gauss the transitions $\Delta m=\pm1, \pm2$ in He and $(F,m)=(1,0)\leftrightarrow(1,-1)$ in H are observed at frequencies of approximately 1570 Mc/sec and 1140 Mc/sec, respectively. The natural line shapes for the separated oscillating fields method are obtained with spacings between the oscillating fields of both 4.2 cm and 2.2 cm. The experimental result is $g_J(\mathrm{He},^3S_1)/g_J(\mathrm{H},^2S_{\frac{1}{2}})|_{\mathrm{exp}}=1-(23.3\pm0.8)\times10^{-6}$, which agrees with an earlier measurement having an accuracy of 16 ppm, and also with the theoretical value $g_J(\mathrm{He},^3S_1)/g_J(\mathrm{H},^2S_{\frac{1}{2}})|_{\mathrm{theor}}=1-(23.3\pm1.0)\times10^{-6}$ obtained by Perl and Hughes, which was computed from the Breit equation for He with the addition of a term to represent the interaction of the anomalous spin magnetic moment of each electron with the external magnetic field.

1. INTRODUCTION

EXTENSIVE experimental tests of the quantum electrodynamic theory of a single electron in external fields have been made through measurements of the Lamb shift in hydrogen[1] and singly ionized helium[2] and of the spin magnetic moment of the electron.[3] The calculated values of the virtual radiative corrections to the energy levels of the electron in external electromagnetic fields have been substantially confirmed by the experiments. For the two-electron system, however, the only critical test of the quantum electrodynamic theory is the measurement of the hyperfine structure of the ground state of positronium.[4] Since it is important to test the basic theory of two interacting electrons as completely as possible, a precision measurement of the magnetic moment of the two-electron system has been undertaken. Specifically, the ratio of the atomic g_J value of helium in its metastable $^3S_1$ state to that of hydrogen in its ground $^2S_{\frac{1}{2}}$ state is determined, and an increase in accuracy of a factor of 20 is obtained in the present experiment compared with an earlier measurement.[5] The magnetic moment of helium in its $^3S_1$ state has been computed from the Breit equation for helium with the addition of a term to represent the interaction of the anomalous spin magnetic moment of each electron with the external magnetic field.[6] This theory of the magnetic interaction energy is believed to be correct to order $\alpha^2\mu_0H_0$ (α=fine structure constant, μ_0=Bohr magneton, and H_0=external magnetic field).

2. THEORY OF EXPERIMENT: LINE SHAPES

The energy levels of helium in its metastable $^3S_1$ state and of hydrogen in its ground $^2S_{\frac{1}{2}}$ state in an external magnetic field have been discussed.[5] At a fixed magnetic field H_0 a Zeeman transition in helium and the transition $(F,m)=(1,0)\leftrightarrow(1,-1)$ (F=quantum number for total atomic angular momentum; m=associated magnetic quantum number) in hydrogen are observed, and from the observed transition frequencies the ratio $g_J(\mathrm{He},^3S_1)/g_J(\mathrm{H},^2S_{\frac{1}{2}})$ is computed. The production and detection of a beam of He atoms in the metastable $^3S_1$ state have also been discussed.[5]

The principal new feature of the present experiment is the use of a transition region with separated oscillating fields.[7] This method of inducing transitions can yield narrow, natural line widths even in the presence of magnetic field inhomogeneities, and hence allows more accurate determinations of the transition frequencies than does the usual resonance method with a single oscillating field.

For hydrogen the transition involves only two energy levels, and the theoretical line shape for a transition induced by separated oscillating fields has been given.[7,8] Assume that the time-dependent perturbation $V(t)$ which induces the transition has matrix elements of the form $V_{pq}=\hbar be^{+i\omega t}$, $V_{qp}=\hbar be^{-i\omega t}$, $V_{pp}=V_{qq}=0$ for the two states p and q. Then the probability that an atom initially in the state p at time $t=0$ will be in the state q at time $t=T+2\tau$ is given by

$$P_{p,q}=4\sin^2\theta\sin^2(a\tau/2)[\cos(\lambda T/2)\cos(a\tau/2)-\cos\theta\sin(\lambda T/2)\sin(a\tau/2)]^2, \quad (1)$$

* This research has been supported in part by the National Science Foundation and by the Air Force Office of Scientific Research.

† Submitted by C. W. Drake in fulfillment of the Ph.D. thesis requirement at Yale University.

‡ Socony Mobil Company Fellow, 1956–1957.

§ Now at I. B. M. Watson Laboratory, New York, New York.

[1] Triebwasser, Dayhoff, and Lamb, Phys. Rev. **89**, 98 (1953); references to the earlier experimental work are given in this paper. The theory is summarized in H. A. Bethe and E. E. Salpeter, *Handbuch der Physik* (Springer-Verlag, Berlin, 1956), Vol. 35.

[2] E. Lipworth and R. Novick, Phys. Rev. **108**, 1434 (1957).

[3] Koenig, Prodell, and Kusch, Phys. Rev. **88**, 191 (1952); R. Beringer and M. A. Heald, Phys. Rev. **95**, 1474 (1954); P. Franken and S. Liebes, Jr., Phys. Rev. **104**, 1197 (1956); C. M. Sommerfield, Phys. Rev. **107**, 328 (1957); Ann. phys. **5**, 26 (1958).

[4] Weinstein, Deutsch, and Brown, Phys. Rev. **94**, 758 (1954); Hughes, Marder, and Wu, Phys. Rev. **106**, 934 (1957); R. Karplus and A. Klein, Phys. Rev. **87**, 848 (1952).

[5] Hughes, Tucker, Rhoderick, and Weinreich, Phys. Rev. **91**, 828 (1953).

[6] W. Perl and V. W. Hughes, Phys. Rev. **91**, 842 (1953).

[7] N. F. Ramsey, Phys. Rev. **78**, 695 (1950).

[8] N. F. Ramsey, *Molecular Beams* (Oxford University Press, London, 1956).

where τ=time spent by the atom in each oscillating field region of length l, and T=time spent by the atom in the intermediate region of length L between the two oscillating field regions.

$$\sin\theta=2b/a,\quad \cos\theta=(\omega_0-\omega)/a,$$
$$a=[(\omega_0-\omega)^2+(2b)^2]^{\frac{1}{2}},\quad \omega_0=(W_q-W_p)/\hbar,$$

in which $W_p(W_q)$ is the energy of the atom in state $p(q)$ in the regions of length l.

$$\lambda=[(\overline{W}_q-\overline{W}_p)/\hbar]-\omega,$$

in which $\overline{W}_p(\overline{W}_q)$ is the space mean value of the energy of the atom in state $p(q)$ over the region of length L. In the actual experiment linearly polarized oscillating magnetic fields are employed, and $V(t)$ is given by

$$V(t)=\mu_0 g_J \mathbf{J}\cdot\mathbf{H}_1\cos\omega t+\mu_0 g_I \mathbf{I}\cdot\mathbf{H}_1\cos\omega t,$$

in which $\mathbf{H}_1$ is perpendicular to $\mathbf{H}_0$. The quantities g_J and g_I are the electronic and nuclear g values $g_J\cong 2$ and $g_I\cong -0.003$. Only the dominant term of $V(t)$, which is the interaction of the oscillating magnetic field with the electronic magnetic moment, need be considered. Furthermore, if the linearly polarized oscillating magnetic field is resolved into two rotating field components, and if only that rotating component which has the proper sense to produce a resonance is retained, then the matrix elements of $V(t)$ are of the form assumed in the derivation of Eq. (1) and $2b=\mu_0 g_J H_1/(2\sqrt{2}\hbar)$. The velocity distribution in the atomic beam is proportional to $v^3\exp[-(v^2/\alpha^2)]$ (α=most probable velocity for an atom in the source), and the average, $\langle P_{p,q}\rangle$, of the transition probability given by Eq. (1) over the beam velocity distribution can be evaluated numerically.

For helium in its $^3S_1$ state, a Zeeman transition involves three equally-spaced energy levels. The theoretical line shapes for transitions induced by separated oscillating fields can be related to the line shape for a transition involving only two levels by use of the Majorana formula,[9]

$$P_{m,m'}=(\cos\tfrac{1}{2}\alpha)^{4J}(J+m)!(J+m')!(J-m)!(J-m')!$$
$$\times\left[\sum_{n=0}^{2J}\frac{(-1)^n(\tan\tfrac{1}{2}\alpha)^{2n-m+m'}}{n!(n-m+m')!(J+m-n)!(J-m'-n)!}\right]^2. \quad (2)$$

$P_{m,m'}$ is the probability that an atom initially in the magnetic substate m will be in the magnetic substate m' at time $t=T+2\tau$. For helium in its $^3S_1$ state the angular momentum quantum number, J, is 1. The quantity $\sin^2(\alpha/2)$ is the transition probability for a system with a spin of $\frac{1}{2}$ and a g value, g_J, equal to that of helium in its $^3S_1$ state. For the method of separated oscillating fields and with a rotating magnetic field of amplitude $H_1/2$,

$$\sin^2(\alpha/2)=P_{\frac{1}{2},-\frac{1}{2}}, \quad (2')$$

in which $P_{\frac{1}{2},-\frac{1}{2}}$ is computed from Eq. (1) with $2b=\mu_0 g_J H_1/(2\hbar)$. The average $\langle P_{m,m'}\rangle$ over the velocity distribution in the beam can be evaluated numerically.

Two different schemes are used for the study of helium Zeeman transitions. The first is the observation of a transition from a particular magnetic substate, for example, $m=+1$, to either of the magnetic substates $m=0$ or $m=-1$. The transition probability is given by

$$P_1=1-P_{1,1}, \quad (3)$$

in which $P_{1,1}$ is given by Eq. (2). The average over the velocity distribution of the beam is

$$\langle P_1\rangle=2\langle P_{\frac{1}{2},-\frac{1}{2}}\rangle-\langle P_{\frac{1}{2},-\frac{1}{2}}{}^2\rangle. \quad (3')$$

The other procedure is the observation of a transition from any of the magnetic substrates $m=0$, $+1$, or -1, to a different final magnetic substrate. If the beam has equal populations of the three magnetic substates, $m=0$, $+1$, and -1, then this transition probability P_T, is given by

$$P_T=\tfrac{1}{3}(1-P_{1,1})+\tfrac{1}{3}(1-P_{0,0})+\tfrac{1}{3}(1-P_{-1,-1}). \quad (4)$$

The average over the velocity distribution of the beam is

$$\langle P_T\rangle=(8/3)\langle P_{\frac{1}{2},-\frac{1}{2}}\rangle-2\langle P_{\frac{1}{2},-\frac{1}{2}}{}^2\rangle. \quad (4')$$

Numerical evaluations of $\langle P_{p,q}\rangle$ for Eq. (1), $\langle P_1\rangle$ of Eq. (3') and $\langle P_T\rangle$ of Eq. (4') have been carried out in the neighborhood of the resonance and are valid provided $(\omega-\omega_0)\ll 2b$. Near resonance the following approximate expressions for $\langle P_{\frac{1}{2},-\frac{1}{2}}\rangle$ [7,8] and $\langle P_{\frac{1}{2},-\frac{1}{2}}{}^2\rangle$ apply:

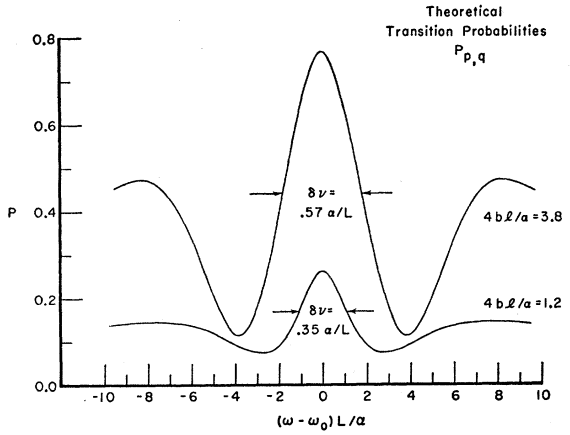

FIG. 1. Transition probability $\langle P_{p,q}\rangle$ as a function of frequency near resonance for the two-level system. Refer to Eq. (1) and accompanying text for definition of l, L, ω, ω_0 and b. The condition $4bl/\alpha=3.8$ corresponds to the optimum amplitude of the oscillating magnetic field required to produce maximum transition probability. The quantity $\delta\nu$ is the frequency width at half-intensity between the peak and the first minima.

[9] E. Majorana, Nuovo cimento **9**, 43 (1932); F. Bloch and I. I. Rabi, Revs. Modern Phys. **17**, 237 (1945).

$$\langle P_{\frac{1}{2},-\frac{1}{2}}\rangle = 2\int_0^\infty \exp(-y^2)y^3 \sin^2\left(\frac{2bl}{\alpha y}\right)\cos^2\left(\frac{\lambda L}{2\alpha y}\right)dy, \quad (5)$$

$$\langle P_{\frac{1}{2},-\frac{1}{2}}{}^2\rangle = 2\int_0^\infty \exp(-y^2)y^3 \sin^4\left(\frac{2bl}{\alpha y}\right)\cos^4\left(\frac{\lambda L}{2\alpha y}\right)dy, \quad (6)$$

where $y=v/\alpha$. These expressions can be written as,

$$\langle P_{\frac{1}{2},-\frac{1}{2}}\rangle = \tfrac{1}{4} - \tfrac{1}{4}I\left(\frac{\lambda L+4bl}{\alpha}\right) - \tfrac{1}{4}I\left(\frac{\lambda L-4bl}{\alpha}\right) + \tfrac{1}{2}I\left(\frac{\lambda L}{\alpha}\right) - \tfrac{1}{2}I\left(\frac{4bl}{\alpha}\right), \quad (5')$$

$$\langle P_{\frac{1}{2},-\frac{1}{2}}{}^2\rangle = \tfrac{9}{64} + \tfrac{3}{8}I\left(\frac{\lambda L}{\alpha}\right) + \tfrac{3}{32}I\left(\frac{2\lambda L}{\alpha}\right) - \tfrac{3}{8}I\left(\frac{4bl}{\alpha}\right) + \tfrac{3}{32}I\left(\frac{8bl}{\alpha}\right) - \tfrac{1}{4}I\left(\frac{4bl+\lambda L}{\alpha}\right) - \tfrac{1}{4}I\left(\frac{4bl-\lambda L}{\alpha}\right) - \tfrac{1}{16}I\left(\frac{4bl+2\lambda L}{\alpha}\right) - \tfrac{1}{16}I\left(\frac{4bl-2\lambda L}{\alpha}\right) + \tfrac{1}{16}I\left(\frac{8bl+\lambda L}{\alpha}\right) + \tfrac{1}{16}I\left(\frac{8bl-\lambda L}{\alpha}\right) + \tfrac{1}{64}I\left(\frac{8bl+2\lambda L}{\alpha}\right) + \tfrac{1}{64}I\left(\frac{8bl-2\lambda L}{\alpha}\right), \quad (6')$$

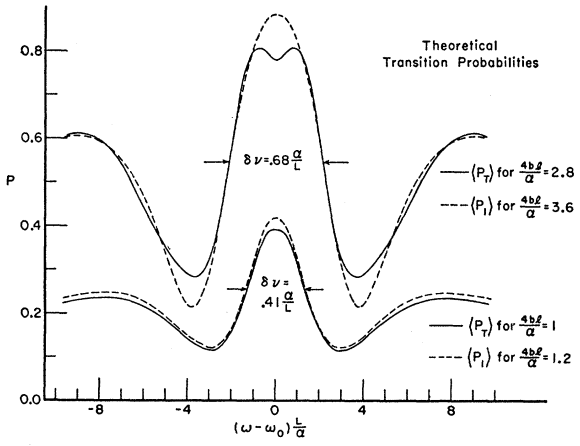

FIG. 2. Transition probabilities $\langle P_1\rangle$ and $\langle P_T\rangle$ as a function of frequency near resonance for the three-level system. $\langle P_T\rangle$ and $\langle P_1\rangle$ are defined for Eqs. (3) and (4). Other quantities are defined for Eq. (1) or in the caption for Fig. 1. The conditions $4bl/\alpha=2.8$ and $4bl/\alpha=3.8$ correspond to amplitudes of the oscillating magnetic field required to produce maximum transition probability for $\langle P_T\rangle$ and $\langle P_1\rangle$, respectively.

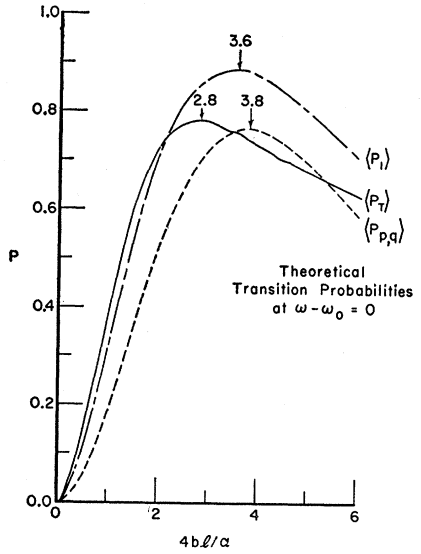

FIG. 3. Transition probabilities at resonance ($\omega_0=\omega$) as a function of the amplitude of the oscillating magnetic field. Symbols are defined in captions for Figs. 1 and 2.

where

$$I(\beta)=\int_0^\infty \exp(-y^2)y^3\cos(\beta/y)dy.$$

A table of the function $I(\beta)$ has been given[10] and can be used to evaluate the above expressions. A table[11] of the related function

$$K(\beta,0,\infty)=\int_0^\infty \exp(-y^2)y^3\sin^2(\beta/2y)dy$$

can also be used.

Curves previously obtained[7,8] for $\langle P_{p,q}\rangle$ near resonance are shown in Fig. 1. Plots for $\langle P_1\rangle$ and $\langle P_T\rangle$ near resonance are shown in Fig. 2. The transition probabilities at resonance ($\omega=\omega_0$) are shown in Fig. 3 as a function of the dimensionless parameter $4bl/\alpha$, which is proportional to the amplitude of the oscillating magnetic field.

3. APPARATUS

A schematic diagram of the essential features of the atomic beam magnetic resonance apparatus is shown in Fig. 4. The vacuum envelope consisted of a brass tube 5 feet in length and 15 inches in diameter, with a cross tube 31 inches in length and 13 inches in diameter in the region of the C magnet. The apparatu swas divided into three chambers—source chamber, interchamber, and main chamber—separately pumped by oil diffusion pumps with speeds of 1400, 300, and 700

[10] V. Kruse and N. F. Ramsey, J. Math. Phys. **30**, 40 (1951); reference 8, Appendix D.

[11] H. Salwen, Phys. Rev. **101**, 621 (1956): Document No. 4716, American Documentation Institute Auxiliary Publication Project, Library of Congress, Washington 25, D. C.

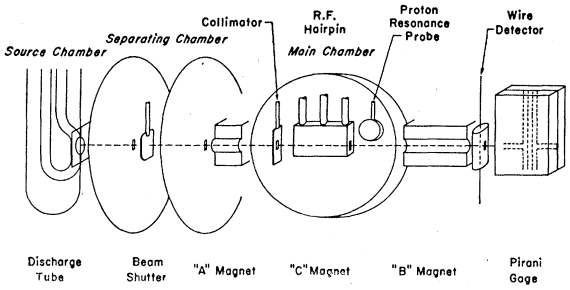

FIG. 4. Schematic diagram of the atomic beam apparatus.

liters/sec, respectively. The three pumps were backed by a 100-liter/sec booster oil pump and a 6-liter/sec mechanical pump. With liquid air cooling and with no flow of gas to the discharge tube, a pressure of 3×10^{-7} mm of Hg was obtained in the main chamber. With a flow of helium gas, the pressures in the main chamber and source chamber were 8×10^{-7} and 3×10^{-5} mm of Hg, respectively; with hydrogen the pressure was about 50% higher in the source chamber.

The source and collimator slits were 0.0125 cm in width, and the height of the beam was limited to 0.3 cm by stops placed on one of the interchamber slits and on the rear of the B magnet. The distance between the source slit and detector was 50 cm.

A movable stop wire, consisting of a 0.125 cm tungsten wire, was located between the C and B fields. It could be positioned to block an undeflected beam and to allow only atoms with a particular sign of magnetic moment to reach the detector.

3.1 Source

The source was a Wood discharge tube[12] similar to that used in the earlier experiment.[5] The discharge tube consisted of a water-cooled 14-mm o.d. glass tube 3 m in length, and of water-cooled aluminum electrodes.[13] The source slit was made from two pieces of quartz ground to give a knife edge and fused together at the top and bottom to form a single plate with a slit of width 0.0125 cm. The quartz plate was waxed on to the discharge tube in the usual manner.[12]

The discharge was excited by a 400-cps ac supply. Typical operating conditions were 240 ma, 2750 volts, and a pressure of 0.1 mm of Hg for helium and 340 ma, 4500 volts, and a pressure of 0.1 mm of Hg for hydrogen. From studies of beam deflection by the inhomogeneous magnetic fields, using the Pirani gauge detector and also the He metastable state detector, it was determined that between 20% and 80% of the particles in the hydrogen beam from the discharge tube were atoms and about one particle in 7×10^4 particles in the helium beam was in the $^3S_1$ metastable state. A dc discharge was tried, using a current-regulated supply which could provide up to 500 ma at 5000 volts. With the dc discharge the atomic hydrogen and metastable helium production was similar to that with the ac discharge, but for helium the photon background noise was larger for the dc discharge than for the ac discharge. Also, the operating conditions for the dc discharge were more critical.

Sputtering of the electrodes resulted in irregular behavior of the discharge, and hence necessitated rather frequent changes of electrodes in the early phase of the experiment. It was found that running an oxygen discharge for about 15 minutes prior to the experiment and the use of a moderately high helium pressure in the discharge resulted in much longer life for the electrodes.[14] Indeed, all final data were taken with one pair of electrodes in a discharge tube which was operated for about 100 hours.

It was noted that the metastable helium atom intensity depended strongly and inversely upon the pressure of helium in the discharge tube. It is presumed that a decrease in pressure increased the production of metastable helium by shifting the mean electron energy toward the maximum of the metastable helium excitation curve, since with the geometry and gas pressures used the loss of metastable atoms in the discharge tube should occur primarily by wall collisions[15] and hence should be more rapid at lower pressures.

3.2 Detectors

Hydrogen atoms were detected with a pirani gauge of the type described by Prodell and Kusch[16] having a slit opening for the beam with a width of 0.0025 cm, a height of 0.33 cm, and a K factor of about 200. The sensitivity was 3.6×10^8 molecules sec^{-1} per mm deflection of a galvanometer with a sensitivity of 0.018 μv/mm at 3 m. The detection time constant was about 7 sec and was determined about equally by the gauge and the galvanometer. Helium atoms in the $^3S_1$ state were detected by electron ejection from a tungsten wire 0.15 mm in diameter and maintained at a negative potential of 22 volts. The electrons were collected by a copper tube 1.9 cm in diameter which surrounded the wire and was near ground potential, and the electron current was measured with an electrometer circuit[17] having a 10^{11} ohm input resistor. If the efficiency for ejection of an electron by a metastable atom[18] is taken as 0.24, the over-all detector sensitivity was 2.6×10^3 metastable atoms sec^{-1} per mm deflection of a galvanometer with a sensitivity of 10^{-10} ampere per mm at 3 m.

[12] Kellogg, Rabi, and Zacharias, Phys. Rev. **50**, 472 (1956).
[13] G. Weinreich and V. W. Hughes, Phys. Rev. **95**, 1451 (1954).
[14] H. S. W. Massey and E. H. S. Burhop, *Electronic and Ionic Impact Phenomena* (Oxford University Press, London, 1952), p. 587.
[15] A. V. Phelps and J. P. Molnar, Phys. Rev. **89**, 1202 (1953); A. V. Phelps, Phys. Rev. **99**, 1307 (1955).
[16] A. G. Prodell and P. Kusch, Phys. Rev. **88**, 184 (1952).
[17] F. Armistead, Rev. Sci. Instr. **20**, 747 (1949).
[18] R. Dorrestein, Physica **9**, 433 (1942); **9**, 447 (1942). H. D. Hagstrum, Phys. Rev. **89**, 244 (1953).

3.3 Magnetic Fields

The A and B magnets were of conventional design for the realization of the two-parallel-wire field with an electromagnet.[8] For the equivalent two-wire field the distance between the wires, $2a$, was 2.3 cm, and hence the ratio of field gradient to field was 0.92 cm^{-1}. The magnets were constructed of soft iron with Permendur pole pieces to prevent local saturation and had high-current windings consisting of water-cooled hollow copper tubing of square cross section 0.66 cm on a side, insulated by unsized Fiberglas sleeving and Teflon sheet. The Fiberglas sleeving was washed in acetone and alcohol before being inserted into the vacuum system and had no adverse effect on the vacuum attained. The A and B magnets each had 19 turns, and were usually operated at 150 amperes, supplied by 3000 ampere-hour submarine batteries, to give a field of 7000 gauss. For a helium atom in the $^3S_1$, $m=\pm 1$ state and having the velocity α each magnet produced a deflection, s_α, of 0.44 mm at the detector. The field gradients of the A and B magnets were in opposite directions so that an atom was refocused if it did not undergo a transition in the C region.

The C magnet, made of Armco soft iron, had circular pole faces 20 cm in diameter and a return yoke of square cross section 7.62 cm on a side. The gap width between the pole faces was 1.27 cm. Adjustable brass spacers placed in the gap allowed for fine adjustment of the parallelism of the pole faces with a variation in spacing of up to 0.1 mm being possible. High-current windings (with 38 turns) similar to those of the A and B magnets were used. The Cmagnet was operated at about 15 amperes to give a field of 550 gauss.

Studies of the magnetic field in the C region were made by the proton magnetic resonance absorption technique, using as a probe a cylindrical glass capsule 1 cm in length and 0.8 cm in diameter containing mineral oil. The A and B magnets produced a field of about 50 gauss at the center of the C-magnet gap, and the homogeneity of the magnetic field in the C region in the horizontal direction along the beam trajectory could be controlled by small-percentage changes in the A- and B-magnet currents which did not appreciably affect the beam deflections. Control of the homogeneity of the magnetic field in the C region in the vertical direction along the beam height was obtained by adjusting the parallelism of the C-magnet pole faces with the brass spacers and could be done with the magnet mounted in the vacuum chamber. Typically, the field inhomogeneities obtained were 6 parts per million (ppm) in a horizontal direction over the 3-mm rf lengths of the loops and the same in a vertical direction over the 3-mm height of the beam.

Regulation of the magnetic field in the C region was achieved electronically by a feedback system which controlled the C-magnet current so as to maintain constant the proton resonance absorption frequency at the probe shown in Fig. 4. The magnetic field regulator consisted of a marginal oscillator[19] with a mineral oil probe followed by a narrow band twin-tee amplifier, a phase detector,[20] and a differential cathode follower which supplied the correction current for the C magnet directly to the high-current magnet windings. The field at the probe was modulated by small coils surrounding the probe shield at a frequency of 44 cps supplied by a Wien Bridge oscillator. A field modulation amplitude of 5 milligauss at the probe had no observable effect on the line shapes obtained from rf induced Zeeman transitions in helium. A field modulation amplitude of 25 milligauss caused an observable broadening of the helium lines.

The regulation only maintained constant the magnetic field at the position of the probe and did not guarantee a constant field at the position of the rf loops. In particular, a change in the A- or B-magnet currents in general resulted in a change in field at the rf loops although the field at the proton probe was maintained constant by the regulator. Thus a one percent change in the A-magnet current caused a change in the helium resonance frequency of 18 ppm, and a one percent change in the B-magnet current caused a change of 90 ppm. The larger effect of a change in the B-magnet current was attributed to the nearness of the B magnet to the proton resonance probe. It was found necessary to monitor the A- and B-magnet currents; this was done manually by varying rheostats so as to maintain constant the voltages across current shunts as read by potentiometers. In this way the A- and B-magnet currents were held constant to one part in 3000 and one part in 30 000, respectively. The value of the C field at the proton probe was locked at a value corresponding to the proton resonance oscillator frequency to within 0.5 to 2 parts in 10^6, depending on the line width of the proton resonance which depended in turn on the local field inhomogeneity over the proton probe and varied from run to run. The proton resonance oscillator frequency was monitored during each run and corrections were made for drifts, which were typically of the order of one part in 10^5 per hour.

3.4 The Radio-Frequency System

A block diagram of the radio-frequency system is shown in Fig. 5. The frequencies used were 1522 and 1608 Mc/sec for the helium transition and 1092 and 1166 Mc/sec for the hydrogen transition. The radio-frequency power was supplied by two shock-mounted, grounded-grid, coaxial-line oscillators using 3C22 lighthouse tubes (radar jammer T85/APT-5). With well-regulated high-voltage supplies and battery-operated filaments these oscillators were stable to within 50 cps.

A multiple of 270 Mc/sec with strong 90 Mc/sec

[19] R. V. Pound and W. D. Knight, Rev. Sci. Instr. **21**, 219 (1950).
[20] N. A. Schuster, Rev. Sci. Instr. **22**, 254 (1951).

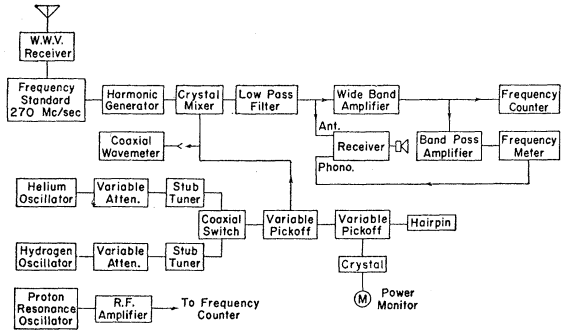

FIG. 5. Block diagram of the radio-frequency system.

side bands was derived from the frequency standard by the harmonic generator and mixed with a signal from the appropriate oscillator to produce a beat between 5 and 15 Mc/sec and also between 80 and 100 Mc/sec. The lower frequency beat could be heard on the receiver for an approximate frequency measurement. The oscillator frequency was measured accurately either by applying the higher frequency beat after wide-band amplification directly to a frequency counter (Hewlett-Packard 524B), or by comparing the lower frequency beat note after video amplification with the output of a frequency meter (BC 221). The latter system was faster and hence was used for most of the data-taking. The accuracy of the frequency measurement was about 5 parts in 10^7.

Two different rf structures were used to produce separated, in-phase oscillating fields. One structure had a separation of 2.2 cm between the two loops and the other (shown in Fig. 6) had a separation of 4.2 cm. Both structures had rf loops of 3-mm wide copper ribbon with a separation transverse to the beam of 1 mm. Each loop was placed in a shield with an inside length of 5 mm in the beam direction. The connections to the rf loops were made with brass coaxial lines of 50 ohms impedance and were brought out of the vacuum through Kovar-to-glass seals.

The rf loops of the shorter 2.2-cm structure were connected together outside the vacuum by type BNC adapters. The two loops could be excited separately and the static magnetic field at each loop could be measured by observing a helium resonance line. In order to minimize the difference in phase between the rf at the two loops the reflection coefficient for each loop was measured with a slotted line and the two reflection coefficients were made equal by a slight movement of one of the loops with respect to its shield. In this way the phase difference was adjusted to be less than 1.5 degrees.

The rf loops "*b*" of the longer 4.2-cm structure (Fig. 6) which provide the separated oscillating fields were connected together inside the vacuum system. The two loops were made identical and the length of the lines from the loops to the connection was short, so that in view of the mechanical tolerances the difference in phase at the two rf loops should be less than 3 degrees. The two separate auxiliary loops "*a*" were used for measuring the magnetic field near each of the loops *b* by observation of a helium resonance line.

To improve the magnetic field homogeneity shimming of the field by use of current loops was employed. Thin three-turn rectangular spirals of $\frac{1}{16}$-inch strip made of 0.001-inch brass stock, and placed between 0.001-inch mica plates were mounted on each rf structure. A 1-cm wide coil over each rf loop on the 2.2-cm structure and a 3.5-cm coil between the rf loops on the 4.2-cm structure were used. Currents between 5 and 50 ma were used.

4. EXPERIMENTAL PROCEDURE

At the start of each run various adjustments of the magnetic fields were made. First the fields at the two rf loops were made equal. This was accomplished by

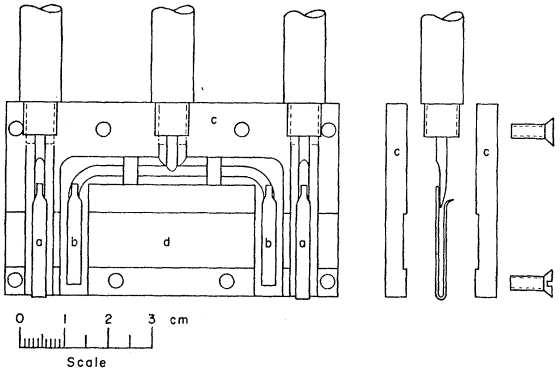

FIG. 6. Diagram of the separated oscillating fields radio-frequency system. The parts labeled "*a*" and "*b*" are the rf current loops of copper ribbon. The loops *b* provide the separated oscillating fields while the auxiliary loops *a* are used to measure the magnetic field. The brass plates "*c*" serve as rf shields for the loops and outer conductor for the coaxial feed to the loops. The groove "*d*" provides the beam path.

observing for helium the broad resonance curves of about 425 kc/sec half-width obtained when the rf loops were separately fed in the 2.2-cm structure (or when the loops *a* were separately fed in the structure of Fig. 6), and by making slight changes (of the order of 3%) in the *A* and *B* currents until the centers of the two resonance curves agreed to within about 25 kc/sec. The total resonance curve was then observed with both rf loops fed in phase, and for many of the runs the central peak in helium was centered in the separated oscillating fields line pattern to within about 25 kc/sec by varying the current (on the order of 20 milliamperes) in the shim coils. A helium resonance line for which the central peak was centered in the line pattern is shown in Fig. 7. Frequently it was necessary to turn the *C*-magnet current on and off several times in order to obtain good field homogeneity over the region of the proton resonance probe, as determined by the transient

effect (wiggles) in the proton resonance signal at high modulation amplitudes. Good field homogeneity at the probe was required in order that the magnetic field regulator operate well at low modulation amplitudes.

The rf power was adjusted to give an intensity for the central peak of about 75% of its maximum value. This adjustment was made for both hydrogen and helium, and the powers were than kept fixed during the run by means of a crystal diode power monitor.

After the above adjustments of the magnetic fields and rf powers were made, resonance curves covering the central region of the line pattern were obtained as shown in Figs. 8 and 9. During the traversal of a resonance line significant changes in background occurred. Hence, customarily, several detector readings were taken with the rf power off during each traversal and were used to correct for the background changes. Resonance lines were taken alternately for hydrogen and helium. Usually the resonance line was traversed in both directions for one gas in about 15 minutes and then a change to the other gas was made. This procedure was repeated until about six changes of gas had been made. Changes in the resonance frequencies with time were observed despite the magnetic field regulation. The changes were due in part to the variation in frequency of the proton resonance oscillator, and corrections for this variation were made in the analysis of the data using observations of the oscillator frequency taken with the frequency counter. Additional slow changes also occurred which were believed to be caused by thermal drifts in the magnets which changed the magnetic field distribution.

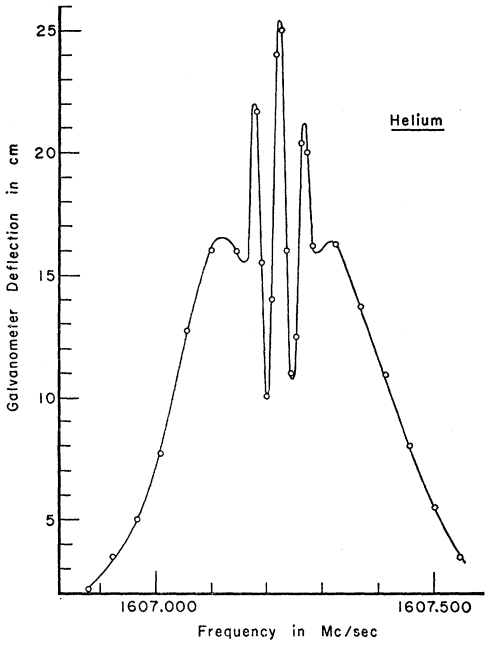

FIG. 7. A complete experimental helium resonance curve taken with separated oscillating fields having a spacing of 4.2 cm between the rf loops. Corrections for zero drift of the detector have been made. One cm of galvanometer deflection corresponds to 10^{-15} ampere.

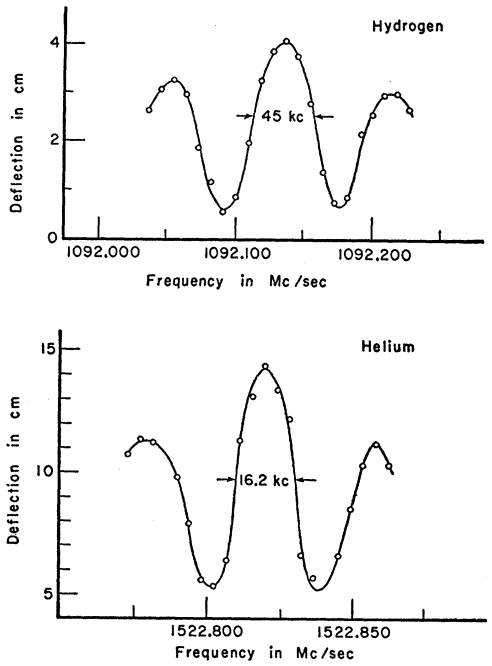

FIG. 8. Typical resonance curves for frequencies near resonance for helium and hydrogen taken with separated oscillating fields of 4.2 cm separation. The hydrogen resonance line is induced with a magnitude of rf magnetic field slightly greater than optimum while the helium resonance line is produced with a magnitude of rf magnetic field such as to produce an amplitude at resonance of about 60% of the maximum value. Corrections for zero drift of the detector have been made.

For hydrogen the background change was principally a uniform, monotonic detector zero drift of about one-tenth the peak signal amplitude over the traversal time. For helium the background change was caused primarily by variation in the light from the discharge tube which ejected electrons from the detector wire.

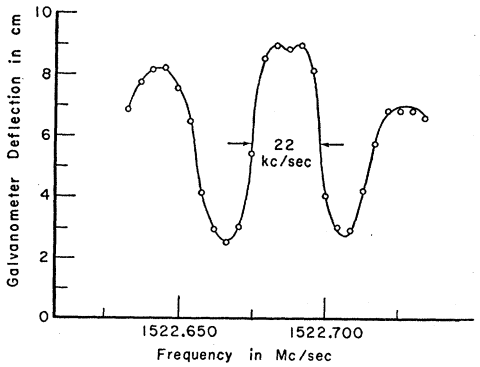

FIG. 9. A helium resonance curve taken for frequencies near resonance with a magnitude of oscillating magnetic field close to the value for maximum transition probability at resonance. The separation between the rf loops was 4.2 cm. Corrections for zero drift of the detector have been made. One cm of galvanometer deflection corresponds to 3×10^{-15} ampere.

This background normally produced about 5 times as much detector signal as that produced by a helium resonance, and the variation in the background was typically $\frac{1}{10}$ to $\frac{1}{5}$ the peak signal amplitude over the transversal time.

In order to avoid systematic errors, data were taken for various changes in the controllable parameters. Two values of magnetic field in the C region—540 gauss and 575 gauss— were used. Most of the data were taken without the use of the wire stop and hence transitions from all the magnetic levels of helium and from both levels of hydrogen were observed. Some data were taken with the use of a wire stop which allowed only one magnetic level of helium and one level of hydrogen to be refocused. Runs were made consecutively for three different beam trajectories obtained by moving the collimator in 0.125-mm steps and realigning the detector for maximum beam intensity with no applied rf power. Data were taken both with and without centering of the central peak in the line pattern. Each rf structure was used in its two possible orientations with respect to the direction of beam propagation.

5. ANALYSIS OF DATA

Typical resonance lines of the central peaks for hydrogen and helium are shown in Figs. 8 and 9. For the hydrogen line of Fig. 8 the rf power was somewhat greater than that needed for maximum line intensity which is given by $4bl/\alpha=3.8$. For the helium line of Fig. 8 the rf power was adjusted to give an intensity for the central peak of about 60% of its maximum value and for the helium line of Fig. 9 the power was adjusted for maximum intensity which is obtained when $4bl/\alpha=2.8$. The experimental hydrogen line of Fig. 8 can be compared with the theoretical line shape of Fig. 1 and the experimental helium lines of Figs. 8 and 9 can be compared with the theoretical line shape $\langle P_T\rangle$ of Fig. 2. The experimental lines agree closely with the theoretical line shapes. In general, the predicted half-widths and peak separations were obtained. The theoretical half-width of the central peak is 38 kc/sec for hydrogen and 22 kc/sec for helium at maximum transition probability with the 4.2-cm rf structure and a source temperature of 300°K.

The resonance frequency for each line was obtained by taking the average of the frequencies of the half-intensity points of the central peak. The observed frequency at the peak of the line in general agreed with the frequency determined from the half-intensity points. The resonance frequency was normally chosen to 500 cps, as determined largely by knowledge of the oscillator frequencies. The resonance frequencies for the lines were then corrected for change of the magnetic field associated with the frequency drift of the proton resonance oscillator. The average resonance frequency for helium (and hydrogen) lines taken before and after a pair of hydrogen (and helium) lines was used, together with the average resonance frequency of the hydrogen (and helium) lines to compute the ratio $g_J(\mathrm{He})/g_J(\mathrm{H})$.

Use of the Breit-Rabi equation for hydrogen[21] and the expression for the Zeeman splitting in helium gives[22]

$$\frac{g_J(\mathrm{He},{}^3S_1)}{g_J(\mathrm{H},{}^2S_{\frac{1}{2}})}=\frac{\nu_{\mathrm{He}}}{\Delta\nu\left[F+\dfrac{k+1}{8F}+\dfrac{(k+1)(k^2-1)}{128F^3}\right]}, \tag{7}$$

where

$$F=\nu_{\mathrm{H}}/\Delta\nu+\tfrac{1}{2},\quad k=\frac{g_J(\mathrm{H},{}^2S_{\frac{1}{2}})/g_I-1}{g_J(\mathrm{H},{}^2S_{\frac{1}{2}})/g_I+1};$$

ν_{He} and ν_{H} are the observed helium and hydrogen resonance frequencies, $\Delta\nu$ (the hyperfine structure separation in hydrogen)$=1420.40573\pm0.00005$ Mc/sec,[23] and $g_J(\mathrm{H},{}^2S_{\frac{1}{2}})/g_I=658.1977\pm0.0009$.[3] The uncertainties in $\Delta\nu$ and in $g_J(\mathrm{H},{}^2S_{\frac{1}{2}})/g_I$ do not significantly affect the calculated value of $g_J(\mathrm{He})/g_J(\mathrm{H})$.

The average of the g-value ratios thus obtained for each run is given in Table I. The root mean square deviation of the g-value ratios obtained in a single run was about 1 ppm. For different runs in which the central peak was centered in the line pattern the average g-value ratios differed by only about 1 ppm.

TABLE I. Results.

Run	Number of resonance lines measured	Magnetic field[a]	Radio-frequency structure[b]	$g_J(\mathrm{He})/g_J(\mathrm{H})$	Relative weight	Deviation from weighted mean value (unit $=10^{-7}$)
1	14	A	I	0.9999775	5	+8
2	14	A	I	0.9999767	5	0
3	14	A	I	0.9999773	5	+6
4	10	A	I	0.9999764	3	−3
5	10	A	I	0.9999725	3	−42
6	10	A	I	0.9999745	3	−22
7	10	A	I	0.9999754	3	−13
8	10	A	I	0.9999763	3	−4
9	10	A	I	0.9999773	3	+6
10	14	B	I	0.9999775	5	+8
11	14	B	I	0.9999756	5	−11
12	18	A	I	0.9999768	7	+1
13	14	A	II	0.9999794	5	+27
14	14	A	II	0.9999811	5	+44
15	14	$A-C$	II	0.9999772	10	+5
16	14	A	II	0.9999778	5	+11
17	10	$A-C$	II	0.9999771	6	+4
18	10	$B-C$	II	0.9999769	6	+2
19	10	B	II	0.9999764	3	−3
20	10	B	II	0.9999746	3	−2
21	14	$B-C$	II	0.9999760	10	−7
22	14	$A-C$	II	0.9999762	10	−5
23	14	$A-C$	I	0.9999777	10	+10

Weighted mean value$=0.9999767$

[a] A—magnetic field such that $f_{\mathrm{He}}=1522$ Mc/sec and $f_{\mathrm{H}}=1092$ Mc/sec; B—magnetic field such that $f_{\mathrm{He}}=1607$ Mc/sec and $f_{\mathrm{H}}=1166$ Mc/sec; C—indicates use of centered separated oscillating fields line pattern (see Sec. 6).

[b] I—2.2-cm rf structure; II—4.2-cm rf structure.

[21] G. Breit and I. I. Rabi, Phys. Rev. **38**, 2082 (1931).

[22] In reference 5 a misprint occurs in the equation on page 837 which should be the same as our Eq. (7).

[23] J. P. Wittke and R. H. Dicke, Phys. Rev. **96**, 530 (1954); P. Kusch, Phys. Rev. **100**, 1188 (1955).

However, for different runs in which the central peak was not centered in the line pattern, the average g-value ratios differed by several ppm. Because of this observed discrepancy as well as for theoretical reasons given in Sec. 6, the runs in which the central peak was centered were assigned a weighting factor two times that of the runs in which the central peak was not centered. The other matter considered in the assignment of a weighting factor for a run was the number of resonance lines taken in the run.

6. SOURCES OF ERROR

Nonconstancy of the magnetic field in the C region was a principal source of error in the experiment. Monitoring of the A- and B-magnet currents limited any error due to change in the A and B fields to about 5 parts in 10^7 for a single g-value ratio determination. Imperfect regulation of the C field which varied greatly from run to run, depending on the width of the proton resonance signal, and drift in frequency of the proton resonance oscillator were the principal causes of random deviations within a single run and could cause a deviation in the g-value ratio of about 2 parts per million.

If the magnetic field at the rf loops is not equal to the average value of the field between the loops, the central peak is not centered in the line pattern and a shift in frequency of the central peak from the true resonance frequency, $(\bar{W}_q-\bar{W}_p)/\hbar$, occurs, which is given by (see Appendix I)

$$d\nu=(\bar{\nu}_0-\nu_0)Gl/L, \tag{8}$$

in which G depends on the value of the rf power and is of the order of 1 for the powers used; the quantity $(\bar{\nu}_0-\nu_0)$ is the difference between the average field between the loops and the common value of the field at the loops, expressed in frequency units. For the 4.2-cm rf structure $l/L=1/15$ and $(\bar{\nu}_0-\nu_0)$ was typically between 50 and 200 kc/sec. The fractional change in g-value ratio is given by

$$dR/R=(d\nu_{\mathrm{He}}/\nu_{\mathrm{He}}-1.155d\nu_{\mathrm{H}}/\Delta\nu)_{\nu_{\mathrm{He}}\sim 1520\ \mathrm{Mc/sec}}, \tag{9}$$

and could amount to as much as 4 parts per million for typical rf field amplitudes. Similar errors can arise with the 2.2-cm rf structure. The relatively large variations in g-value ratios obtained from runs in which the central peak was not centered in the line pattern (see Table I) are believed due to this effect. In the histogram of the results shown in Fig. 10 all values outside of the limits ± 10 parts in 10^7 of the average value are due to runs in which the central peak was not centered. Since the rf powers vary from run to run, the g-value ratios should vary randomly from run to run, and indeed the average g-value ratio obtained from the uncentered runs agrees with the value obtained from the centered runs. If the central peak of the separated rf field line pattern is set to be within 20 kc/sec of the center of the broad peak, the error in the g-value ratio will be less than about 8 parts in 10^7.

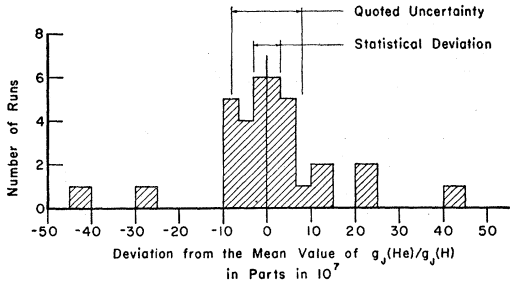

FIG. 10. Histogram of experimental data for the ratio $g_J(\mathrm{He})/g_J(\mathrm{H})$. The value zero on the abscissa corresponds to the weighted mean value of all the experimental data.

The measurements of the g-value ratio for various beam positions in the C-field region were done to ascertain whether field inhomogeneities introduced any error due to the slightly different trajectories for hydrogen and helium and they indicated no appreciable systematic variations.

A difference in phase between the two rf fields causes[24] a shift in frequency of the central peak by the amount $d\nu\cong(\delta\nu)(\Delta\phi)/\pi$, where $\delta\nu$ is the frequency half-width of the central peak and $\Delta\phi$ is the phase difference in radians. For $\Delta\phi=0.03$ radian, which was the maximum value indicated by tests on the 2.2-cm rf structure, an error in the g-value ratio of about 5 parts in 10^7 results. A reversal of the rf structure with respect to the direction of beam propagation should result in an error of the opposite sign. Both rf structures were used with both orientations and no systematic differences in the g-value ratio were observed.

The error in picking the center of the line due to source and detector noise was estimated to be about 1 kc/sec. An error of about 500 cps in a single rf frequency measurement was possible due to the noise band width of the frequency standard ($\sim$300 cps) and the calibration error of the frequency meter (about 200 cps). No significant error can arise from the frequency standard since it was calibrated daily against radio station WWV to several parts in 10^7, and since further any error in the frequency standard is greatly reduced in the computation of the g-value ratio.

7. RESULTS

The results for all the runs are listed in Table I. The average g-value ratio for the six runs in which the central peak was centered in the line pattern was $g_J(\mathrm{He},{}^3S_1)/g_J(\mathrm{H},{}^2S_{\frac{1}{2}})=1-(23.2\times10^{-6})$ with a standard deviation of 0.3×10^{-6}. The average of all other runs (17 in number) was $g_J(\mathrm{He},{}^3S_1)/g_J(\mathrm{H},{}^2S_{\frac{1}{2}})=1-(23.4\times10^{-6})$, with a standard deviation of 0.3×10^{-6}. The over-all average of all the data give $g_J(\mathrm{He},{}^3S_1)/g_J(\mathrm{H},S_{\frac{1}{2}})=1-(23.3\times10^{-6})$, with a standard deviation of

[24] N. F. Ramsey and H. B. Silsbee, Phys. Rev. 84, 506 (1951).

0.25×10^{-6}. Reasonable variations in the assigned weighting factor do not change the results by more than a few parts in 10^7. The final result is $g_J(\mathrm{He},{}^3S_1)/g_J(\mathrm{H},S_{\frac{1}{2}})=1-(23.3\pm0.8)\times10^{-6}$, where the stated uncertainty is three times the standard deviation.

It is believed that the ratio $g_J(\mathrm{He})/g_J(\mathrm{H})$ could be measured to an accuracy of one part in 10^7 or better with certain modifications in the experiment described in this paper. The principal modification would be the use of a higher value of the C field so that the resonance frequencies occur at about 10 000 Mc/sec. Since the natural line width is independent of the field value, a substantial increase in the ratio of resonance frequency to line width can be expected. Improvement in the control and homogeneity of the fields would be necessary and are believed possible.

8. DISCUSSION OF RESULTS

The theory of atomic magnetism based on a Dirac-Breit equation for helium with the addition of a term to represent the interaction of the anomalous spin moment of each electron with the external magnetic field gives,[6] for the ${}^3S_1$ state,

$$\begin{aligned} g_J(\mathrm{He},{}^3S_1)&=2(1+\alpha/2\pi-0.328\alpha^2/\pi^2 \\ &\quad -\tfrac{1}{3}\langle T\rangle/mc^2-\tfrac{1}{6}\langle e^2/r_{12}\rangle/mc^2) \\ &=2(1+1161.4\times10^{-6}-1.8\times10^{-6} \\ &\quad -38.7\times10^{-6}-2.3\times10^{-6}) \\ &=2(1.0011186), \end{aligned} \tag{10}$$

in which $\langle T\rangle$ is the expectation value for the kinetic energy of the electrons and $\langle e^2/r_{12}\rangle$ is the expectation value of the electrostatic interaction between the two electrons. The term $(\alpha/2\pi-0.328\alpha^2/\pi^2)$ is the contribution of the anomalous spin magnetic moment of the electron.[25] The term involving $\langle T\rangle$ is a relativistic bound state correction similar to that in hydrogen.[26] The term involving $\langle e^2/r_{12}\rangle$ is a correction arising from the Breit interaction.[27] Use of the theoretical g value[25,26] for hydrogen, $g_J(\mathrm{H},1^2S_{\frac{1}{2}})=g_s(\mathrm{free})(1-\alpha^2/3)=2(1.0011419)$, together with Eq. (10) gives

$$g_J(\mathrm{He},{}^3S_1)/g_J(\mathrm{H},{}^2S_{\frac{1}{2}})\big|_{\mathrm{theor}} =1-[(23.3\pm1.0)\times10^{-6}]. \tag{11}$$

The uncertainty is assigned to account for the neglect of virtual radiative terms of order α.[3] The g-value ratio obtained in this experiment is

$$g_J(\mathrm{He},{}^3S_1)/g_J(\mathrm{H},{}^2S_{\frac{1}{2}})\big|_{\mathrm{exp}} =1-[(23.3\pm0.8)\times10^{-6}], \tag{12}$$

in excellent agreement with the theoretical value.

If the experimental value[28] $g_J(\mathrm{H},{}^2S_{\frac{1}{2}})=2(1.001139\pm0.000010)$ is used together with Eq. (12), one obtains $g_J(\mathrm{He},{}^3S_1)=2(1.001116\pm0.00010)$, where the uncertainty arises from the measured value of g_l/g_p. If the theoretical value of $g_J(\mathrm{H},{}^2S_{\frac{1}{2}})$ is used together with the experimental value of $g_J(\mathrm{He},{}^3S_1)/g_J(\mathrm{H},{}^2S_{\frac{1}{2}})$ given in Eq. (12), one obtains $g_J(\mathrm{He},{}^3S_1)=2(1.0011186\pm0.0000012)$ in agreement with the theoretical value of Eq. (10).

The agreement provides strong confirmation of the theory of the relativistic contributions to atomic magnetism as based on the Dirac-Breit equation to order $\alpha^2\mu_0H_0$, and confirms that the anomalous magnetic moments of the two electrons in helium are additive to this order. The measurement also provides a test for any more rigorous theory of atomic magnetism for helium based on the Bethe-Salpeter equation.[29]

The excellent agreement of theory and experiment for helium justifies confidence in the relativistic theory of atomic magnetism for multielectron atoms based on a generalized Dirac-Breit equation[30] and hence indicates that the magnetic moments of more complex atoms can be calculated to order $\alpha^2\mu_0$ if sufficiently good atomic wave functions are available. Conversely, the experimental value of an atomic magnetic moment can serve as a test for the excellence of an atomic wave function.

APPENDIX I

In this appendix the shift in frequency of the central peak of the line pattern obtained by the method of separated oscillating fields from the true resonance is computed for the case in which the field at the rf loops is not equal to the average field between the loops. Use the notation[7,8] $\bar{\omega}_0=(\bar{W}_q-\bar{W}_p)/\hbar$ and $\omega_0=(W_q-W_p)/\hbar$, in which W_p and W_q refer to the energy levels at the positions of the rf loops and $\bar{W}_p$ and $\bar{W}_q$ refer to the space-average energy levels in the region between the rf loops. Assume $\bar{\omega}_0\neq\omega_0$. Then in the neighborhood of the resonance peak where $\lambda T/2\ll1$ and $(\omega_0-\omega)/2b\ll1$, Eq. (1) reduces to

$$\begin{aligned} P_{pq}&=4S^2C^2[1-y^2-(S/C)2b\tau x^2 \\ &\quad -2\sqrt{2}(S/C)xy+(C/S)2b\tau x^2-2x^2], \end{aligned} \tag{13}$$

in which $y=\lambda T/2$, $x=(\omega_0-\omega)/(2b)$, $S=\sin b\tau$, and $C=\cos b\tau$. This expression has its maximum value at

[25] J. Schwinger, Phys. Rev. **73**, 416 (1948); R. Karplus and N Kroll, Phys. Rev. **77**, 536 (1950); C. M. Sommerfield, Phys. Rev. **107**, 328 (1957) and Ann. phys. **5**, 26 (1958).

[26] G. Breit, Nature **122**, 649 (1928); H. Margenau, Phys. Rev. **57**, 383 (1940); N. F. Mott and H. S. W. Massey, *The Theory of Atomic Collisions* (Clarendon Press, Oxford, 1949), second edition, p. 72.

[27] G. Breit, Phys. Rev. **34**, 553 (1929); **39**, 616 (1932).

[28] This number is computed from the unweighed averages of the two measurements of $g_J(\mathrm{H},{}^2S_{\frac{1}{2}})/g_p$ and of the two measurements of g_l/g_p given in reference 3. The quantity g_l is the orbital g value of the free electron.

[29] E. E. Salpeter and H. A. Bethe, Phys. Rev. **84**, 1232 (1951); M. Gell-Mann and F. Low, Phys. Rev. **84**, 350 (1951); H. Araki, Progr. Theoret. Phys. (Japan) **17**, 619 (1957).

[30] W. Perl, Phys. Rev. **91**, 852 (1953); A. Abragam and J. H. Van Vleck, Phys. Rev. **92**, 1448 (1953).

$\omega=\tilde{\omega}_0+d\omega$, where

$$d\omega=(\tilde{\omega}_0-\omega_0)Gl/L, \tag{8'}$$

in which

$$G=\frac{\tan b\tau+l/L[\tan b\tau-\cos b\tau+1/(b\tau)]}{2l/L\,\tan b\tau+b\tau+(l/L)^2[\tan b\tau-\cos b\tau+1/(b\tau)]}.$$

For $l/L=1/15$ and for values of $4b\tau$ between 1 and 5, G is between 0.9 and 2.0. If $(\tilde{\omega}_0-\omega_0)/2\pi=100$ kc/sec, $d\omega/2\pi$ is between 6 and 12 kc/sec.

Consideration of the velocity distribution of the beam and of the case of a system with three equally-spaced energy levels (helium) is not expected to change the order of magnitude of the above estimate.

PHYSICAL REVIEW VOLUME 112, NUMBER 5 DECEMBER 1, 1958

Effects of an Electric Dipole Moment of the Electron on the Hydrogen Energy Levels*

G. FEINBERG
Brookhaven National Laboratory, Upton, New York

(Received July 18, 1958)

The bound states in a Coulomb field of a charged, spin $\frac{1}{2}$, particle with an electric dipole moment are obtained. The nonrelativistic Schrödinger equation for such a particle is solved in closed form. The wave functions are generalizations of the Coulomb wave functions, involving Laguerre polynomials of nonintegral upper index. The accidental degeneracies of the Coulomb energy levels are removed by the dipole interaction. In particular, there will be an additional contribution to the splitting between the $2S_{\frac{1}{2}}$ and $2P_{\frac{1}{2}}$ states coming from the dipole moment. By requiring that this extra energy shift should not destroy the agreement between the theoretical and experimental values of the Lamb shift, it is found that the dipole moment of the electron must be less than 10^{-13} cm times the electron charge. Other effects of the dipole moment on the hydrogen energy levels are discussed.

I. INTRODUCTION

THE possible existence of electric dipole moments for the spin $\frac{1}{2}$ elementary particles has been the subject of some recent theoretical and experimental investigation. Theoretically, it has been shown that the invariance of physical laws under space reflection or time reversal would imply the nonexistence of such moments,[1] provided that there is no more degeneracy of the states of a free spin $\frac{1}{2}$ particle at rest than that given by the two spins and the particle-antiparticle.[2] Experimentally, there is a very accurate measurement of the neutron electric dipole moment through a magnetic resonance method.[3] This indicates that the electric dipole moment of the neutron is less than 5×10^{-20} cm times the electron charge. There do not seem to be any such accurate limits known for the dipole moments of charged particles such as electrons. In view of some recent experiments which have been interpreted as indicating that the positron has a large dipole moment,[4] it seems useful to see what limits for the electron dipole moment are implied by the measurements of the hydrogen energy levels by Lamb and others.[5] In particular, one may expect that the $2S_{\frac{1}{2}}$ and $2P_{\frac{1}{2}}$ states, which are split only by radiative corrections to the Dirac equation, would further be split by the interaction of an electric dipole moment with the Coulomb field, and so the dipole moment must be small enough so as not to spoil the agreement between the experimental value of this splitting and the value predicted by quantum electrodynamics. The dependence of the splitting on the dipole moment will be obtained in Sec. II, where the nonrelativistic Schrödinger equation for a charged particle, with a dipole moment, in a Coulomb field is solved in closed form. The energy levels depend only on the square of the dipole moment, as would be expected from a perturbation calculation. The energy levels and wave functions obtained are used in Sec. III to discuss the limits on the dipole moment of the electron implied by various measurements on the hydrogen atom.

II. WAVE FUNCTIONS FOR A PARTICLE WITH AN ELECTRIC DIPOLE MOMENT IN A COULOMB FIELD

We consider the Schrödinger equation for a nonrelativistic charged particle with an electric dipole

* Work performed under the auspices of the U. S. Atomic Energy Commission.

[1] Lee, Oehme, and Yang, Phys. Rev. **106**, 340 (1957).

[2] The requirement of the lack of degeneracy has been stressed by N. F. Ramsey, Phys. Rev. **109**, 225 (1958). If there exist spin $\frac{1}{2}$ particles with two otherwise degenerate states for each value of the spin, momentum, and charge, and these states have opposite but nonvanishing electric dipole moment, then the definition of space reflection and time reversal may be extended so that these states are transformed into each other under these operations, and the invariance of the Hamiltonian will be maintained. The particles which constitute ordinary matter, i.e., the electron, neutron and proton, presumably cannot be of this type, because such an added degeneracy would change the form of the periodic table and the nuclear shell structure by allowing twice as many particles into each closed shell.

[3] Smith, Purcell, and Ramsey, Phys. Rev. **108**, 120 (1957).

[4] F. E. Obenshain and L. A. Page, Phys. Rev. **112**, 179 (1958).

[5] Triebwasser, Dayhoff, and Lamb, Phvs. Rev. **89**, 98 (1953).